

Effect of Viscous Unsteady Aerodynamics on Flutter Calculation

Haithem Taha* and Amir S. Rezaei[†] and Mohamed Mahmoud[‡]
University of California, Irvine, CA 92697

Many studies over the 1960's reported failure in predicting accurate flutter boundaries using the classical theory of unsteady aerodynamics even at zero angle of attack and/or lift conditions. Since the flutter phenomenon lies in the intersection between unsteady aerodynamics and structural dynamics, and because the structural dynamics of slender beams can be fairly predicted, it was inferred that the problem stems from the classical theory of unsteady aerodynamics. As a result, a research flurry occurred over the 1970's and 1980's investigating such a theory, with particular emphasis on the applicability of the Kutta condition to unsteady flows. There was almost a consensus that the Kutta condition must to be relaxed at high frequencies and low Reynolds numbers, which was also concluded from several recent studies of the unsteady aerodynamics of bio-inspired flight. Realizing that vorticity generation and lift development are essentially viscous processes, we develop a viscous extension of the classical theory of unsteady aerodynamics, equivalently an unsteady extension of the boundary layer theory. We rely on a special boundary layer theory that pays close attention to the details in the vicinity of the trailing edge: the triple deck theory. We use such a theory to relax the Kutta condition and determine a viscous correction to the inviscid unsteady lift. Using the developed viscous unsteady model, we develop a Reynolds-number-dependent lift frequency response (i.e., a viscous extension of Theodorsen's). It is found that viscosity induces a significant phase lag to the lift development beyond Theodorsen's inviscid solution, particularly at high frequencies and low Reynolds numbers. Since flutter, similar to any typical hopf bifurcation, is mainly dictated by the phase difference between the applied loads and the motion, it is expected that the viscosity-induced lag will affect the flutter boundary. To assess such an effect, we couple the developed unsteady viscous aerodynamic theory with a structural dynamic model of a typical section to perform aeroelastic simulation and analysis. We compare the flutter boundary determined using the developed viscous unsteady model to that of Theodorsen's.

I. Introduction

Wing flutter is a crucial limit that confines the flight envelope of an airplane. It is a truly multidisciplinary phenomenon that lies in the intersection between aerodynamics and structure dynamics. That is, a model for one of these two disciplines cannot alone capture the physics of the phenomenon. There must be a representative model for each discipline. The aerodynamic loads provide a negative damping for the structural deflections, which increases with the airplane speed. As such, beyond a certain speed, the aerodynamic negative damping outweighs the structural positive damping resulting in flutter instability.

The structural dynamics of high aspect ratio wings can be fairly predicted using the Euler-Bernoulli beam theory¹ or its geometrically exact version.^{2,3} On the other side, while the steady aerodynamics of wings at small angles of attack and high Reynolds numbers is well established (e.g., the vortex lattice method⁴), it is well-known that the flutter is a highly unsteady aeroelastic phenomenon. That is, a quasi-steady aerodynamic model usually results in a flutter boundary away from the actual limit. For example, the unsteady added mass terms lead to a significant increase in the flutter speed: since increasing the structure mass (virtually in this case) delays flutter.¹ Moreover, the lag concomitant with the unsteady aerodynamic loads plays a

^{*}Assistant Professor, Mechanical and Aerospace Engineering, AIAA Member.

[†]PhD Student, Mechanical and Aerospace Engineering, AIAA Student Member.

[‡]Visiting Undergraduate Student from the Aerospace Engineering Department at Cairo University, Egypt.

crucial role in dictating the flutter boundary. Note that the flutter instability, similar to any typical hopf bifurcation, is mainly dictated by when energy is added/subtracted during the cycle. That is, the phase difference between the applied loads (aerodynamic loads) and the motion plays a crucial role in dictating the stability boundary. In fact, even small changes in this phase difference (by say 10 degrees) leads to a significant change in the flutter boundary.^{1,5}

Unfortunately, the unsteady aerodynamics of wings or even two-dimensional airfoils does not enjoy the same maturity as the steady counterpart or the structural dynamics theory. Tracing the origin of the classical theory of unsteady aerodynamics, we find that it is mainly based on Prandtl's assumption: for infinitely thin airfoils at small angles of attack and high Reynolds numbers, separation or sheets of vorticity are shed from the sharp edges only and the flow outside of these sheets can be modeled using inviscid assumptions.^{6,7} These concepts, in addition to assuming small disturbance to the mean flow (flat wake assumption), form the heart of the classical theory of unsteady aerodynamics, which has been extensively utilized throughout the years. In 1925, Wagner⁸ used this formulation to solve the indicial problem (lift response due to a step change in the angle of attack). In 1935, Theodorsen⁹ used the same formulation to solve the frequency response problem (steady state lift response due to harmonic oscillation in the angle of attack) and applied it to the analysis of wing flutter. In 1938, Von Karman and Sears¹⁰ provided a more general and elaborate representation of the classical formulation. Also, the efforts of Kussner¹¹ for the sharp edged gust problem, Schwarz¹² for the frequency response problem, and Lowey¹³ for the returning wake problem worth mentioning. In addition to the classical developments, Prandtl's formulation provides the basis for many recent developments. 14-27 However, this framework using potential flow is not complete and invokes a closure or auxiliary condition (e.g., the Kutta condition). This potential flow formulation cannot alone determine the amount of shed vorticity at the trailing edge, which is a very crucial quantity as it determines the circulation bound the airfoil (via conservation of circulation), which in turn dictates the generated lift force.

The most common auxiliary condition used in literature is the Kutta condition whose application to steady flows has been very successful. However, its application to unsteady flows has been controversial (see Crighton²⁸ and the references therein). The need for an auxiliary condition alternative to Kutta's goes as early as the work of Howarth²⁹ with a research flurry on the applicability of Kutta condition to unsteady flows in the 1970's and 1980's. 28, 30-33 This research was mainly motivated by the failure to capture an accurate flutter boundary. 34-36 Since flutter simply lies in the intersection between unsteady aerodynamics and structural dynamics, and because the structural dynamics theory is in a much better status (vibration of slender beams can be accurately predicted using the exact beam theory for example), it has been deemed that the flaw stems from the classical unsteady aerodynamic theory, particularly the Kutta condition, as suggested by Chu³⁷ and Shen and Crimi³⁸ among others. Moreover, since these deviations occurred even at zero angle of attack (or lift), ^{39,40} it was inferred that there is a fundamental issue with such a theory that is not merely a higher-order effect due to nonlinearities at high angles of attack.³⁷ Therefore, there was almost a consensus that the Kutta condition has to be relaxed particularly at large frequencies, large angles of attack and/or low Reynolds numbers. 32, 41, 42 In fact, Orszag and Crow 43 regarded the full-Kutta-condition solution as "indefensible". Interestingly, this dissatisfaction of the Kutta condition and the need for its relaxation is recently rejuvenated with the increased interests in the low Reynolds number, high frequency bio-inspired flight. 17, 44-47

We note that the whole issue about the Kutta condition stems from the fact that it provides a remedy for an inviscid theory of unsteady lift whereas the vorticity generation and lift development are essentially viscous processes. To relax the Kutta condition, we recently developed a viscous extension of the classical theory of unsteady aerodynamics, ^{5,48} equivalently, an unsteady extension of the viscous boundary layer theory. It is based on a special boundary layer theory that pays close attention to the details in the vicinity of the trailing edge where the Blasius boundary layer interacts with the Goldstein near wake layer. Our viscous extension resulted in a Reynolds number dependent extension of Theodorsen's lift frequency response. It was found that the viscous correction induces a significant phase lag to the circulatory lift component, particularly at low Reynolds numbers and high-frequencies, that matches high-fidelity simulations of Navier-Stokes and previous experimental results. ^{33,36,40,49} This enhancement in the predicted phase of the unsteady loads is expected to affect the flutter calculation as discussed above, which is the main motivation behind this work.

In this paper, we summarize the developed viscous unsteady aerodynamic model. Based on which, we present a modified (viscous) Theodorsen function that depends on the Reynolds number. We then couple this harmonic representation of the viscous unsteady aerodynamic forces with the standard structural dynamics of a typical section¹ to determine the effect of viscosity-induced lag on the flutter boundary.

II. Viscous Unsteady Aerodynamic Model

A. Background: The Triple Deck Boundary Layer Theory

In the early 1900, Prandtl has formulated the well-known boundary layer equations:⁵⁰ nonlinear partial differential equations that approximate Navier-Stokes equations in the thin viscous layer around the airfoil. In 1908, Blasius⁵¹ solved this set of equations over a flat plate at zero angle of attack subject to the noslip boundary condition on the plate, which lead to the celebrated Blasius boundary layer solution. Later (in 1930), Goldstein⁵² solved the same boundary layer equations of Prandtl in the wake region behind the plate, replacing the no-slip condition with a zero-stress condition on the wake center line. He found that the removal of the wall accelerates the flow leading to a favorable pressure gradient. That is, near the trailing edge, there are two boundary layers interacting with each other, as shown in Fig. 1: the Blasius boundary layer, whose thickness is of order $R^{-1/2}$, and Goldstein near-wake, whose thickness is scaled as $R^{-1/2}x^{1/3}$ where R is the Reynolds number and x is the distance downstream of the edge. 28 The triple deck theory has been devised to model such local interactions near the trailing edge of a flat plate in steady flow. In contrast to the classical boundary layer theory where only the normal coordinate is scaled, the tangential coordinate is also scaled (zoomed) in the triple deck theory to resolve such interactions. Scaling dictates that the transition region between the two layers takes place over a short length of order $R^{-3/8}$ (as shown in Fig. 1), which is similar to Lighthill's supersonic shock-wave-boundary-layer interaction.⁵³ In conclusion, the triple deck theory represents a solution to the discontinuity of the viscous boundary condition at the edge:⁵⁴ from a zero tangential velocity on the airfoil to a zero pressure discontinuity on the wake center line.

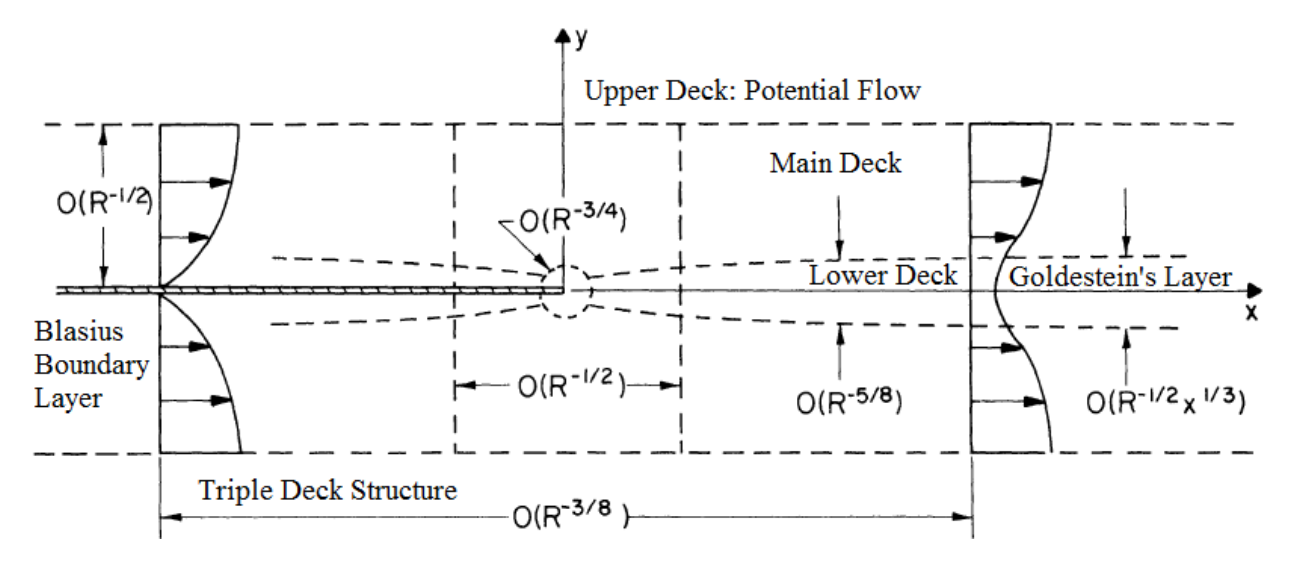


Figure 1: Triple deck structure and various flow regimes. Adapted from Messiter. 55

Aerodynamicists modeled this transition through three decks (triple deck theory): (i) the upper deck which constitutes of an irrotational flow outside of the main boundary layer, (ii) the main deck which constitutes the main boundary layer (Blasius), and (iii) the lower deck, which is a sub-layer inside the main boundary layer, as shown in Fig. 1. Stewartson⁵⁶ and Messiter⁵⁵ were the first to develop the triple deck theory for a flat plate in a steady flow at zero angle of attack. Their efforts resulted in the the following correction of the Blasius skin friction drag coefficient

$$C_D \simeq \frac{1.328}{\sqrt{Re}} + \frac{2.66}{Re^{7/8}},$$

which is in an astonishingly good agreement with both Navier-Stokes simulations and experiments down to R=10 and even lower. Brown and Stewartson⁵⁷ extended the work of Stewartson⁵⁶ and Messiter⁵⁵ to the case of small but non-zero angle of attack α_s , in the order of $R^{-1/16}$. This range is of interest because (i) if α_s is much smaller, then the flow can be considered as a perturbation to the case of $\alpha_s=0$ and (ii) if it is much larger, then the flow would separate well before the trailing edge. Over this range, the resulting adverse pressure gradient is of the same order as the favorable pressure gradient in the triple deck, leading

to separation in the immediate vicinity of the trailing edge, which is called *Trailing Edge stall*. Brown and Stewartson⁵⁷ formulated such a problem and showed that the flow in the lower deck is governed by partial differential equations that are solved numerically for each value of $\alpha_e = R^{1/16} \lambda^{-9/8} \alpha_s$, where $\lambda = 0.332$ is the Blasius skin-friction coefficient. Chow and Melnik⁵⁸ solved the triple deck boundary layer equations in the case $0 < \alpha_e < 0.45$ and concluded that the flow will separate from the suction side of the airfoil from the trailing edge at $\alpha_e = 0.47$ (trailing edge stall angle). We remark that this α_e value for trailing edge stall corresponds to quite a small value for the actual angle of attack; $\alpha = 3.1^{\circ} - 4.2^{\circ}$ for $R = 10^{4} - 10^{6}$.

Brown and Stewartson⁵⁷ wrote the steady pressure distribution near the trailing edge ($\hat{x} = 1$) as

$$P_s(\hat{x} \to 1) = \rho U^2 \alpha_s \left[-\sqrt{\frac{1-\hat{x}}{2}} + \frac{B_s/2}{b\sqrt{\frac{1-\hat{x}}{2}}} \right] \operatorname{sgn}(y),$$
 (1)

where ρ is the fluid density, U is the free-stream, $\operatorname{sgn}(y)$ is positive on the upper surface, α is the angle of attack and B_s is the trailing edge singularity term, which is supposed to be zero according to the Kutta condition. In contrast, it is determined by matching the triple deck with the outer flow. The numerical solution by Chow and Melnik⁵⁸ provides B_e as a nonlinear function of α_e , which is represented here in Fig. 2, where

$$\alpha_e = \alpha_s \epsilon^{-1/2} \lambda^{-9/8} \text{ and } B_s = 2b\epsilon^3 \lambda^{-5/4} B_e(\alpha_e).$$
 (2)

In other words, Fig. 2 and Eq. (2) provides the trailing edge singularity B_s as a nonlinear function of the angle of attack α_s in a steady flow.

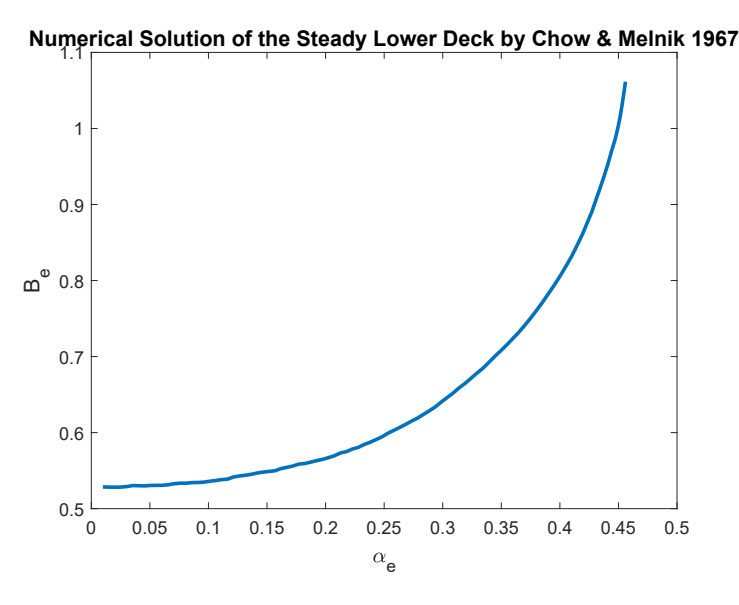


Figure 2: Numerical solution of the steady lower deck equations for $0 < \alpha_e < 0.45$, adapted from Chow and Melnik.⁵⁸

B. Viscous Unsteady Lift Frequency Response Using Triple Deck Theory

Brown and Daniels⁵⁴ were the first to extend the steady triple deck theory to the case of an oscillatory pitching flat plate. Unlike the steady case, there is a Stokes layer near the wall that is of order $\sqrt{\nu/\omega}$ where the viscous term is balanced by the time-derivative term in the equations. Brown and Daniels considered the impractical, yet mathematically-appealing, case of very high-frequency $k = O(R^{1/4}) = \frac{1}{\epsilon^2}$ and very small amplitude $O(R^{-9/16})$, where k is the reduced frequency. Luckily, focusing on the more practical case of $0 < k << Re^{1/4}$ and $\alpha = O(R^{-1/16})$ results in vanishing the time-derivative term in both the the main deck and lower deck equations as shown by Brown and Cheng.⁵⁹ Therefore, the boundary layer equations look the same as those governing the steady case at a non-zero α_s (studied by Brown and Stewartson⁵⁷) with a proper definition for the equivalent steady angle of attack. However, we emphasize that this approach is not a quasi-steady solution; although the time-derivative does not show up in the lower deck equations, the

correspondence with the steady equations implies an equivalent angle of attack that is dependent on the oscillation frequency, as will be shown below. Therefore, the lower deck system is dynamical (i.e., possesses a non-trivial frequency response).

In our recent efforts, 5,48 we have developed a viscous extension of the classical theory of unsteady aerodynamics using the triple deck theory results (discussed above). For an arbitrarily deforming thin airfoil in the presence of a uniform stream U, the inviscid pressure distribution is typical written as 1,60,61

$$P(\theta, t) = \rho \left[\frac{1}{2} a_0(t) \tan \frac{\theta}{2} + \sum_{n=1}^{\infty} a_n(t) \sin n\theta \right], \tag{3}$$

where θ is the tangential angular coordinate along the plate (0 at trailing edge and π at the leading edge). Each term in the series (3) automatically satisfies the Kutta condition (zero loading at the trailing edge). The pressure on the lower side is given by the negative of Eq. (3). The no-penetration boundary condition will provide a means to determine all the coefficients a_n 's (except a_0) in terms of the plate motion kinematics as shown by Robinson and Laurmann, ⁶¹ pp. 491. For example, for a pitching-plunging flat plate, as shown in Fig. 3, the normal velocity of the plate (assuming small disturbances \dot{h} and α) is written as

$$v_p(x,t) = \dot{h}(t) - \dot{\alpha}(t)(x - ab) - U\alpha, \quad -b \le x \le b, \tag{4}$$

where b is the half-chord length, h is the plunging displacement (positive upward), α is the pitching angle (angle of attack, positive clockwise), and ab represents the chordwise distance from the mid point to the hinge point, as shown in Fig. 3. This type of kinematics results in

$$a_1(t) = b\dot{v}_{1/2} - bU\dot{\alpha}(t), \quad a_2(t) = -\frac{b^2\ddot{\alpha}(t)}{4}, \quad \text{and} \quad a_n = 0 \ \forall n > 2,$$
 (5)

where $v_{1/2}$ is the normal velocity at the mid-chord point, which is given by

$$v_{1/2}(t) = \dot{h}(t) + ab\dot{\alpha}(t) - U\alpha.$$

The determination of a_0 (leading edge singularity term) is more involved in the sense that it requires solving an integral equation, which cannot be solved analytically for arbitrary time-varying wing motion. It has been solved for some common inputs, e.g., step change in the angle of attack resulting in the Wagner's response, simple harmonic motion resulting in Theodorsen's frequency response, and sharp-edged gust. Theodorsen's harmonic solution implies, a_0 pp. 496 a

$$a_0(t) = U \left[2V_{3/4}C(k)e^{i\omega t} + b\dot{\alpha}(t) \right], \tag{6}$$

where $v_{3/4}(t) = V_{3/4}e^{i\omega t}$ is the normal velocity at the three-quarter-chord point, and C(k) is the Theodorsen's frequency response function, which depends on the reduced frequency $k = \frac{\omega b}{U}$ as

$$C(k) = \frac{H_1^{(2)}(k)}{H_1^{(2)}(k) + iH_0^{(2)}(k)},\tag{7}$$

where $H_n^{(m)}$ is the Hankel function of m^{th} kind of order n. In the common classification proposed by Theodorsen, the coefficient a_0 represents the circulatory contribution while the other two coefficients a_1 , a_2 represent the non-circulatory contribution. Finally, the potential-flow lift force and pitching moment (positive pitching up) at the mid-chord point are written as

$$L_P = -\pi \rho b(a_0 + a_1)$$
 and $M_{0_P} = \frac{\pi}{2} \rho b^2 (a_2 - a_0)$. (8)

Following Brown and Stewartson,⁵⁷ we added a trailing edge singularity term to the inviscid unsteady pressure distribution (3) whose strength will be determined from the triple deck theory

$$P(\theta, t) = \rho \left[\frac{1}{2} a_0(t) \tan \frac{\theta}{2} + \sum_{n=1}^{\infty} a_n(t) \sin n\theta + \frac{1}{2} B_{\mathbf{v}}(t) \cot \frac{\theta}{2} \right]. \tag{9}$$

^aNote that the presentation of Robinson and Laurmann is adapted to a more common and modern notation.

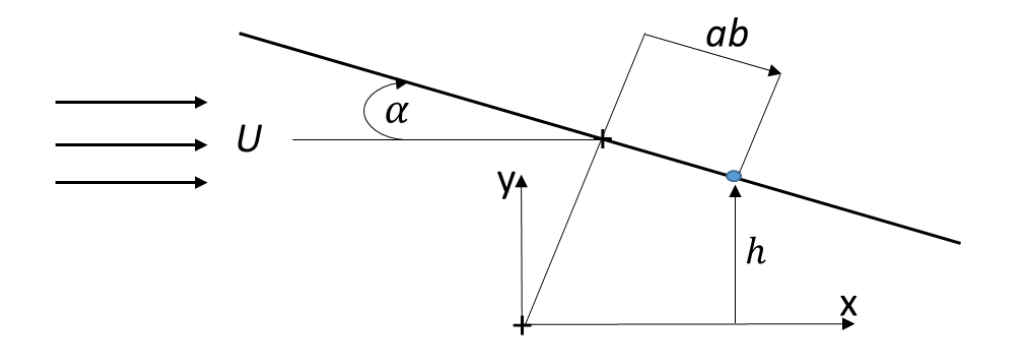


Figure 3: A schematic diagram for an oscillating flat plate.

It should be emphasized that the no-penetration boundary condition, alone, cannot determine $B_{\rm v}$ and an auxiliary condition is invoked to determine its value within the framework of potential flow. In particular, the Kutta condition dictates that $B_{\rm v}=0$ resulting in the potential-flow solution introduced above. In our recent effort, ^{5,48} we used the unsteady triple deck theory, exploiting the vanishing of the time-derivative term from the boundary layer equations, to determine $B_{\rm v}$ in terms of k and k. Then, the viscous unsteady lift and pitching moment will be written as

$$L = -\pi \rho b(a_0 + a_1 + B_v)$$
 and $M_0 = \frac{\pi}{2} \rho b^2 (a_2 - a_0 + B_v)$. (10)

To determine the viscous correction $B_{\rm v}$ of the pressure distribution, consider approaching the trailing edge $(\theta \to 0 \text{ or } \hat{x} = \frac{x}{b} \to 1)$, the pressure distribution is then written as

$$P(\hat{x} \to 1; t) = \rho \left[\left(\frac{1}{2} a_0(t) + 2 \sum_{n=1}^{\infty} n a_n(t) \right) \sqrt{\frac{1 - \hat{x}}{2}} + \frac{B_{\mathbf{v}}(t)/2}{\sqrt{\frac{1 - \hat{x}}{2}}} \right], \tag{11}$$

which has the same form as the steady distribution given in Eq. (1) with

$$\alpha_s(t) \equiv \frac{1}{U^2} \left| \frac{1}{2} a_0(t) + 2 \sum_{n=1}^{\infty} n a_n(t) \right| \text{ and } B_{\mathbf{v}}(t) \equiv -\left(\frac{1}{2} a_0(t) + 2 \sum_{n=1}^{\infty} n a_n(t) \right) \frac{B_s(t)}{b},$$
 (12)

where α_s and B_s are the equivalent steady angle of attack and trailing edge singularity term, respectively. This comparison along with the fact that the time-derivative term does not enter the triple deck equations points to the possibility of directly using the steady solution by Chow and Melnik⁵⁸ of the inner deck equations for the unsteady case with the equivalence shown above, valid in the range $0 < k < O(R^{1/4})$. In the above equivalence, if the term $\frac{1}{2}a_0(t) + 2\sum_{n=1}^{\infty}na_n(t)$ is negative, then the top of the oscillating thin airfoil will correspond to the top of the steady plate and if is positive, then the top of the oscillating thin airfoil should correspond to the bottom of the steady plate. In either case, α_s would be positive.

For a harmonically oscillating flat plate at a given reduced frequency k and Reynolds number R, the coefficients a_0 , a_1 , and a_2 of the inviscid pressure distribution are given in Eqs. (5,6). Thus, α_s can be obtained accordingly from Eq. (12). Care should be taken when applying Eq. (12). It should be applied instantaneously: at each time instant, the right hand side containing the a's coefficients is complex because a_0 contains the complex-valued function C(k). The instantaneous $\alpha_s(t)$ should be given by

$$\alpha_s(t) = \frac{1}{U^2} \left| \Re \left[\frac{1}{2} a_0(t) + 2a_1(t) + 4a_2(t) \right] \right|,$$

where $\Re(.)$ denotes the real part of its complex argument. As such, the equivalent angle of attack $\alpha_e(t)$ for the numerical solution of Chow and Melnik⁵⁸ is obtained from Eq. (2) with $\epsilon = R^{-1/8}$. Note that if $\alpha_e(t)$ exceeds 0.47, then the simulation should be terminated because such a value implies trailing edge stall beyond which the current analysis is not valid. Using, Fig. 2, one can obtain $B_e(t)$, which in turn is

substituted in Eq. (2) to determine B_s and consequently the viscous correction $B_v(t)$ from Eq. (12). Finally, the unsteady viscous circulatory lift coefficient is written as

$$C_{L_C}(t) = \Re \left[2\pi \alpha_{3/4}(t)C(k) - \pi \hat{B}_{v}(t) \right],$$
 (13)

where $\alpha_{3/4}$ is the local angle of attack at the three-quarter-chord point, as recommended by Pistolesi theorem, ⁶⁰ pp. 80. A spectral analysis (e.g., FFT) is applied to $C_{L_C}(t)$ to extract its relative amplitude and phase shift with respect to the quasi-steady lift coefficient: $C_{L_{QS}}(t) = 2\pi\alpha_{3/4}(t)$. That is, the circulatory-lift viscous transfer function $C_{\rm v}$ is defined as

$$C_{\rm v}(k;R) \triangleq \frac{C_{L_C}(k;R)}{C_{L_{QS}}(k)}.$$

Figure 4 shows a block diagram for the dynamics of the unsteady viscous circulatory lift.

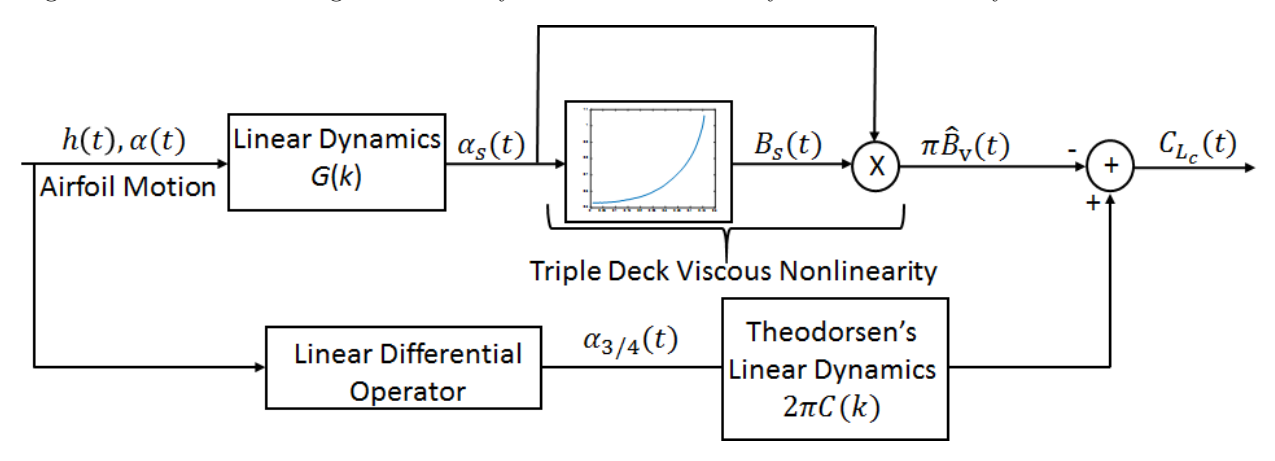


Figure 4: A block diagram showing the different components constituting the dynamics of the viscous circulatory lift.

Following the above procedure, we recently constructed a Reynolds number dependent lift frequency response, 5,48 which is shown in Fig. 5 in comparison to Theodorsen's. Intuitively, as R increases, the viscous response approaches the inviscid Theodorsen's response and vice versa. In particular, viscosity leads to a significantly more phase lag than Theodorsen's at high reduced frequencies and lower Reynolds numbers, which is in agreement with our computational simulations 5,48,62 and the simulations of Othman et al. 63 For example, Fig. 6 (a) shows a comparison for the pressure distribution over a flat plate using the inviscid theory, the current viscous theory, and computational simulations in the case of a harmonically pitching airfoil about its quarter-chord with 3 ° amplitude at $R=10^{5}$, k=1. The figure shows the pressure distribution at the instant of maximum effective angle of attack (maximum $\dot{\alpha}$). The resulting pressure distribution from the developed viscous theory well matches the URANS computational results. Moreover, Fig. 6 (b) provides a comparison for the viscous phase frequency response at $R=10^{5}$, 10^{4} , which also shows a good matching between the developed theory and higher-fidelity simulations.

The obtained phase results are also in accordance with the experimental results of Chu and Abramson, ⁴⁰ Henry, ³⁶ Abramson and Ransleben, ⁴⁹ and Bass et al. ³³ In these experimental efforts, the authors reconciled the deviation between Theodorsen's prediction of the unsteady aerodynamic loads and their measurements by adding some suggested phase lag to Theodorsen function, which is naturally captured in the developed viscous theory. This result is particularly important for flutter calculation. Note that the flutter instability, similar to any typical hopf bifurcation, is mainly dictated by when energy is added/subtracted during the cycle. That is, the phase difference between the applied loads (aerodynamic loads) and the system motion (e.g., angle of attack) plays a crucial role in dictating the stability boundary. Therefore, if Theodorsen's model does not capture such a phase lag accurately, it may lead to a deviation in the flutter boundary. As such, it is expected that the developed viscous frequency response will result in a more accurate, yet efficient, estimate of the flutter boundary, which is the main subject of the current study. For more details about the physics behind the observed viscosity-induced lag and its relation with the Kutta condition, the reader is referred to the effort.⁵

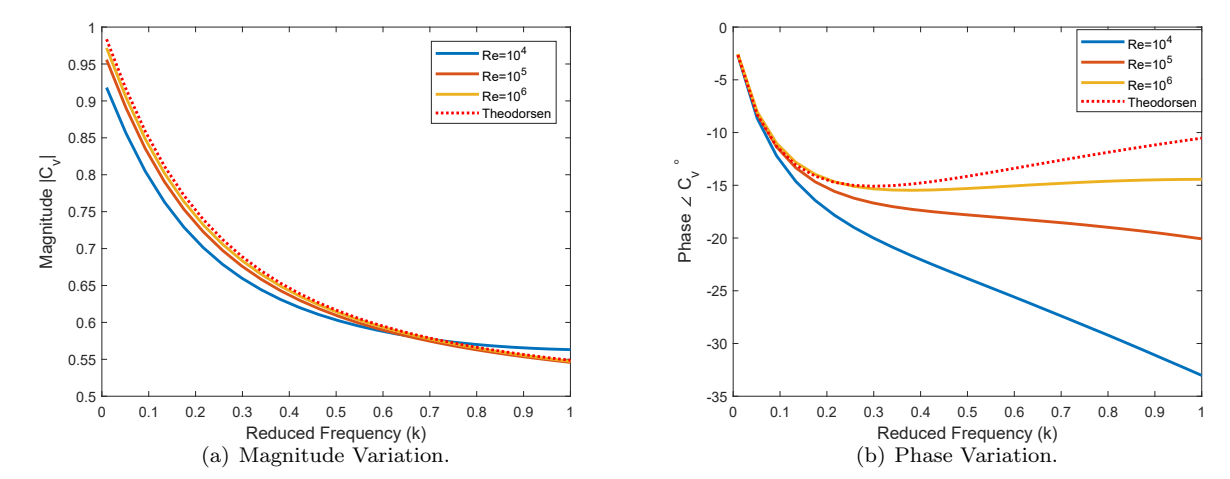


Figure 5: Comparison between the frequency responses of the unsteady, viscous, circulatory lift coefficient C_{L_C} at different Reynolds numbers and that of the potential-flow circulatory lift coefficient (i.e., Theodorsen's). Adopted from 5,48

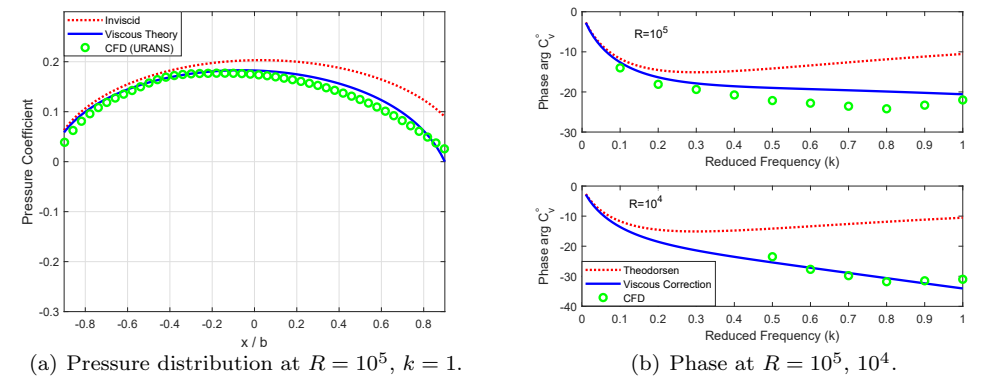


Figure 6: Validation of the pressure distribution and circulatory lift frequency response phase.

III. Aeroelastic Modeling

The structural dynamic model of a typical section undergoing pitching-plunging motion is written as

$$\begin{bmatrix} m & -mbx_{\alpha} \\ -mbx_{\alpha} & I_{\alpha} \end{bmatrix} \begin{pmatrix} \ddot{h} \\ \ddot{\alpha} \end{pmatrix} + \begin{bmatrix} K_{h} & 0 \\ 0 & K_{\alpha} \end{bmatrix} \begin{pmatrix} h \\ \alpha \end{pmatrix} = \begin{pmatrix} L \\ M_{h} \end{pmatrix}, \tag{14}$$

where m is the mass of the section, bx_{α} is the offset of the section center of gravity (cg) behind its shear center (SC) as shown in Fig. 7, I_{α} is the section pitching moment of inertia about the shear center, K_h and K_{α} are the plunging and pitching stiffness, respectively, and M_h is the pitching moment at the shear center point. Equation (14) can be written in the abstract form

$$[\boldsymbol{M}_s]\ddot{\boldsymbol{q}} + [\boldsymbol{K}_s]\boldsymbol{q} = \boldsymbol{Q}_a, \tag{15}$$

where $\mathbf{q} = (h, \alpha)$ is the vector of generalized coordinates, and \mathbf{M}_s and \mathbf{K}_s are the mass and stiffness matrices of the structure dynamics. Although, we use a typical section in this paper, the analysis is valid for a three-dimensional linear structural model (e.g., Euler Bernoulli). The mass and stiffness matrices will be simply replaced by those of the beam finite element model.

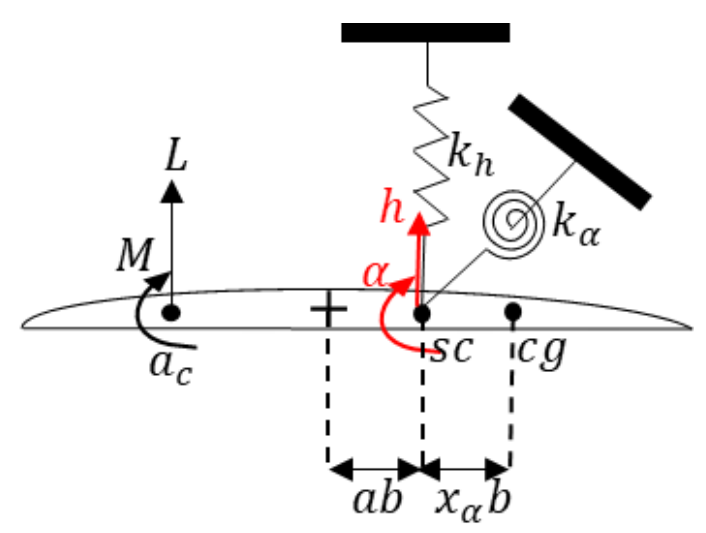


Figure 7: A schematic diagram for a typical section: pitching and plunging stiffness are represented by simple springs.

The viscous contribution $B_{\rm v}$ to the lift can be classified as a circulatory effect leading to a modified (viscous) Theodorsen function $C_{\rm v}(k;R)$, which is shown in Fig. 5, or a non-circulatory effect leading to a reduction in the added mass, as demonstrated in our earlier effort.⁵ As far as the lift force is concerned, one can proceed with either choice. Since the former is more convenient (allows using the obtained viscous transfer function $C_{\rm v}(k;R)$ in place of Theodorsen), it is adopted the following lift representation

$$L = L_{QS}C_{v}(k;R) + L_{NC} = \underbrace{-2\pi\rho U b v_{3/4} C_{v}(k;R)}_{\text{Circulatory}} + \underbrace{-\pi\rho b^{2} \dot{v}_{1/2}}_{\text{Non-circulatory}}.$$
 (16)

However, the same approach cannot be adopted in the moment representation because the lift viscous contribution $L_{\rm v}=-\pi\rho bB_{\rm v}$ does not act at the same point as the inviscid circulatory contribution. It is known that the latter acts at the quarter-chord point.¹ In contrast, Eq. (10) implies that the viscous contribution acts at the three-quarter-chord point. Hence, one can write the unsteady aerodynamic moment at the shear center as

$$M_{h} = \underbrace{L_{QS}C(k)b\left(\frac{1}{2} + a\right)}_{\text{Circulatory}} + \underbrace{L_{NC}ab}_{\text{Non-circulatory}} + \Delta M + \underbrace{-L_{v}b\left(\frac{1}{2} - a\right)}_{\text{Viscous Contribution}}, \tag{17}$$

where $\Delta M = -\frac{\pi}{8}\rho b^3 \left(4U\dot{\alpha} + b\ddot{\alpha}\right)$ per Theodorsen's theory. Realizing that $L_{\rm v} = L_{QS}\left[C_{\rm v}(k;R) - C(k)\right]$, Eq. (17) can be simplified as

$$M_h = L_{QS}b\tilde{C}(k;R) + L_{NC}ab + \Delta M, \tag{18}$$

where $\tilde{C} = C - C_{\rm v} \left(\frac{1}{2} - a\right)$.

In order to couple the developed viscous unsteady aerodynamic model with a structural model for an aeroelastic analysis, we have to present the aerodynamic loads in terms of the structural degrees of freedom (airfoil motion): $q = [h, \alpha]$. Using Eqs. (16,18), we can write the unsteady aerodynamic loads as

$$Q_a = -[M_a]\ddot{q} - [D_a]\dot{q} - [K_a]q, \tag{19}$$

where the aerodynamic mass, damping, and stiffness matrices are given by

$$\boldsymbol{M}_{a} = \pi \rho b^{2} \begin{bmatrix} 1 & ab \\ ab & b^{2} \left(a^{2} + \frac{1}{8}\right) \end{bmatrix}, \ \boldsymbol{D}_{a} = 2\pi \rho U b \begin{bmatrix} C_{v} & -b \left[C_{v} \left(\frac{1}{2} - a\right) + \frac{1}{2}\right] \\ b\tilde{C} & b^{2} \left(\frac{1}{2} - a\right) \left(\frac{1}{2} - \tilde{C}\right) \end{bmatrix}, \ \boldsymbol{K}_{a} = -2\pi \rho U^{2} b \begin{bmatrix} 0 & C_{v} \\ 0 & b\tilde{C} \end{bmatrix}.$$

Coupling the structural model (15), equivalently (14), with the aerodynamic model (19), as shown in Fig. 8, we write the free aeroelastic system as

$$\underbrace{[\boldsymbol{M}_s + \boldsymbol{M}_a]}_{\boldsymbol{M}} \ddot{\boldsymbol{q}} + [\boldsymbol{D}_a(U, k)] \dot{\boldsymbol{q}} + \underbrace{[\boldsymbol{K}_s + \boldsymbol{K}_a]}_{\boldsymbol{K}(U, k)} \boldsymbol{q} = \boldsymbol{0}. \tag{20}$$

Since the focus is on the flutter boundary, one can assume a simple harmonic motion $q = \bar{q}e^{i\omega t}$, where \bar{q} represents the flutter mode shape. As such, Eq. (20) implies

$$\underbrace{\left[-\omega^2 M + i\omega D_a(U,k) + K(U,k)\right]}_{\mathbf{A}_{ab}} \bar{q} = \mathbf{0}.$$
(21)

A non-zero solution for \bar{q} is only possible when the aeroelastic system matrix A_{ae} is singular. Hence, the aeroelastic stability can be easily studied via the condition

$$\det \left[\mathbf{A}_{ae} \right] = \det \left[-\omega^2 \mathbf{M} + i\omega \mathbf{D}_a(U, k) + \mathbf{K}(U, k) \right] = 0.$$
(22)

This equation can be normalized by dividing the first equation by $\pi \rho b^3$ and the second line by $\pi \rho b^4$, to obtain

$$\det \begin{bmatrix} 1+\mu & -\mu x_{\alpha}+a \\ -\mu x_{\alpha}+a & \mu r_{\alpha}^{2}+a^{2}+\frac{1}{8} \end{bmatrix} - \frac{2i}{k} \begin{bmatrix} C_{\mathbf{v}}(k;R) & -C_{\mathbf{v}}(k;R) \left(\frac{1}{2}-a\right)-\frac{1}{2} \\ \tilde{C}(k;R) & \left(\frac{1}{2}-a\right)\left(\frac{1}{2}-\tilde{C}(k;R)\right) \end{bmatrix} - \begin{bmatrix} \mu \frac{\omega_{h}^{2}}{\omega_{\alpha}^{2}}\chi & -2\frac{C_{\mathbf{v}}}{k^{2}} \\ 0 & \mu \chi r_{\alpha}^{2}-2\frac{\tilde{C}}{k^{2}} \end{bmatrix} = 0,$$

$$\hat{\mathbf{M}}$$

$$(23)$$

where the over hat denotes normalized quantity, $\mu = \frac{m}{\pi \rho b^2}$ is the ratio between the airfoil mass and the added (virtual) mass, $r_{\alpha} = \sqrt{\frac{I_{\alpha}}{m}}$ is the section radius of gyration about the shear center, $\omega_h = \sqrt{\frac{K_h}{m}}$ and $\omega_{\alpha} = \sqrt{\frac{K_{\alpha}}{I_{\alpha}}}$ are the plunging and pitching natural frequencies, respectively, and $\chi = \frac{\omega_{\alpha}^2}{\omega^2}$, which is unknown. The left hand side of Eq. (23) is usually referred to as the flutter determinant.

The algebraic condition (23) results in two equations (because it is complex-valued) in the two unknowns k, χ , given the section non-dimensional parameters μ , a, x_{α} , $\frac{\omega_h}{\omega_{\alpha}}$, and r_{α} . They are typically solved via iterative techniques such as the u-g method or the p-k method 1 to determine the flutter reduced frequency k_F and the non-dimensional flutter speed $\frac{U_F}{b\omega_{\alpha}} = \frac{1}{k_F\sqrt{\chi_F}}$. However, in this case where the viscous transfer function C_v depends on the Reynolds number, the situation is more involved; for a non-dimensional problem, a Reynolds number must be assumed. For a dimensional problem, a double-iteration loop will be required. That is, a value for R will be assumed to solve for $\frac{U_F}{b\omega_{\alpha}}$ and consequently the flutter speed U_F . The Reynolds number would then be updated based on the computed flutter speed.

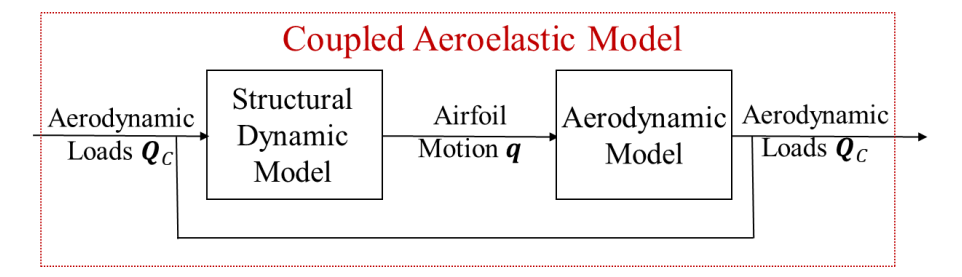


Figure 8: A schematic diagram that shows the coupling between the aerodynamic and structural dynamics models.

IV. Simulation Results: Effect of Viscosity on Flutter Calculation

To assess the effect of viscosity and its associated phase lag on flutter, we compare the resulting flutter boundary from the condition (22), which is based on the developed viscous unsteady aerodynamic theory, with the inviscid flutter boundary based on Theodorsen's theory. The latter can be determined from the condition (22) by setting $C_{\rm v}(k;R) = C(k)$ and $\tilde{C}(k;R) = C(k)\left(\frac{1}{2}+a\right)$. Also, the quasi-steady flutter boundary can be obtained by neglecting all the non-circulatory contributions and setting $C_{\rm v}(k;R) = 1$. In this case, one must at least retain the moment term $\Delta M = -\frac{\pi}{2}\rho b^3 U\dot{\alpha}$, which is reminiscent of the steady solution of a pitching flat plate using thin airfoil theory. For comparison purposes, the following empirical formula by Theodorsen and Garrick⁶⁴ is included

$$\frac{U_F}{b\omega_\alpha} = \sqrt{\frac{\mu r_\alpha^2}{1 + 2(a + x_\alpha)}}$$

We studied the effect of the section parameters μ , a, x_{α} , $\frac{\omega_h}{\omega_{\alpha}}$ on the inviscid and viscous flutter boundaries as well as the quasi-steady one. For this steady, the following nominal values are used

$$\mu = 4, \quad \frac{\omega_h}{\omega_\alpha} = \frac{1}{2}, \quad r_\alpha = 0.5$$

Figures 9, 10 show the resulting effects of μ , $\frac{\omega_h}{\omega_\alpha}$, a, and x_α on different estimates of the flutter boundary. When studying one parameter, the others are held at the nominal values. Because the problem is sensitive to variations of a or x_α , they are treated differently (no nominal values).

The results in Figs. 9, 10 show that the quasi-steady estimate is quite off, which is well known. The flutter boundary predicted by the developed viscous theory is mostly closer to the empirical formula than Theodorsen's inviscid boundary. And a large values of the mass ratio μ , all three estimates become close. However, the viscous boundary is consistently lower than Theodorsen's inviscid boundary, which is a serious finding that necessitates further validation with higher-fidelity (computational or experimental) simulations. The implication is that Theodorsen's boundary is misleading, indicating a seemingly higher flutter boundary, which would jeopardize the designs of flying vehicles based on it (they can be susceptible to flutter). It may be important to note that a value of $R = 10^6$ is assumed in this analysis along with a turbulent viscosity ratio of 10; i.e., a value of $R = 10^5$ is used in the simulations of the viscous theory.

This issue is made clearer in the following dimensional case of

$$\mu = 2.97, \ a = 0, \ \frac{\omega_h}{\omega_\alpha} = 0.59, \ b = 3 \ ft, \ \text{and} \ \omega_\alpha = 14.81 \ rad/s$$

where a double iteration loop is performed to iterate on the Reynolds number. Table 1 shows a comparison among the flutter predictions using quasi-steady aerodynamics, Theodorsen's inviscid unsteady model, 9 and the viscous unsteady aerodynamic model developed above at different values of x_{α} . Since the shear center is at the mid-chord point (a=0), then x_{α} represents the distance between the mid-chord point and the center of gravity normalized by the half-chord length b. A larger x_{α} means a more backward cg, which is expected to lead to an earlier flutter (i.e., lower flutter speed and higher flutter reduced frequency) according to the empirical formula above.

This trend is confirmed in the results of Table 1. As x_{α} increases, the flutter speed, U_F , decreases and the flutter reduced frequency, k_F , increases. The quasi-steady estimate is way off the unsteady estimates,

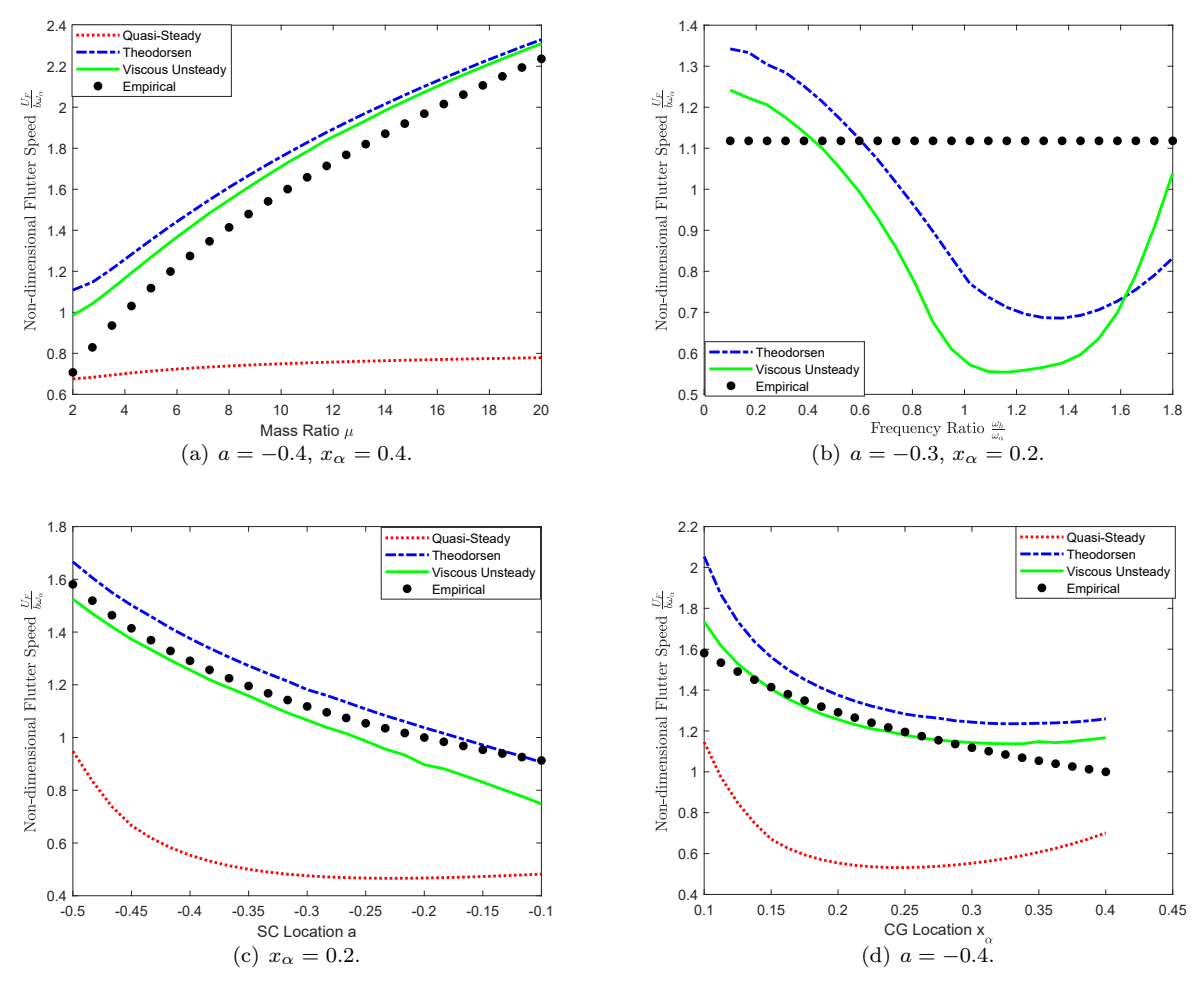


Figure 9: Variation of flutter non-dimensional speed $\frac{U_F}{b\omega_{\alpha}}$ with the section parameters.

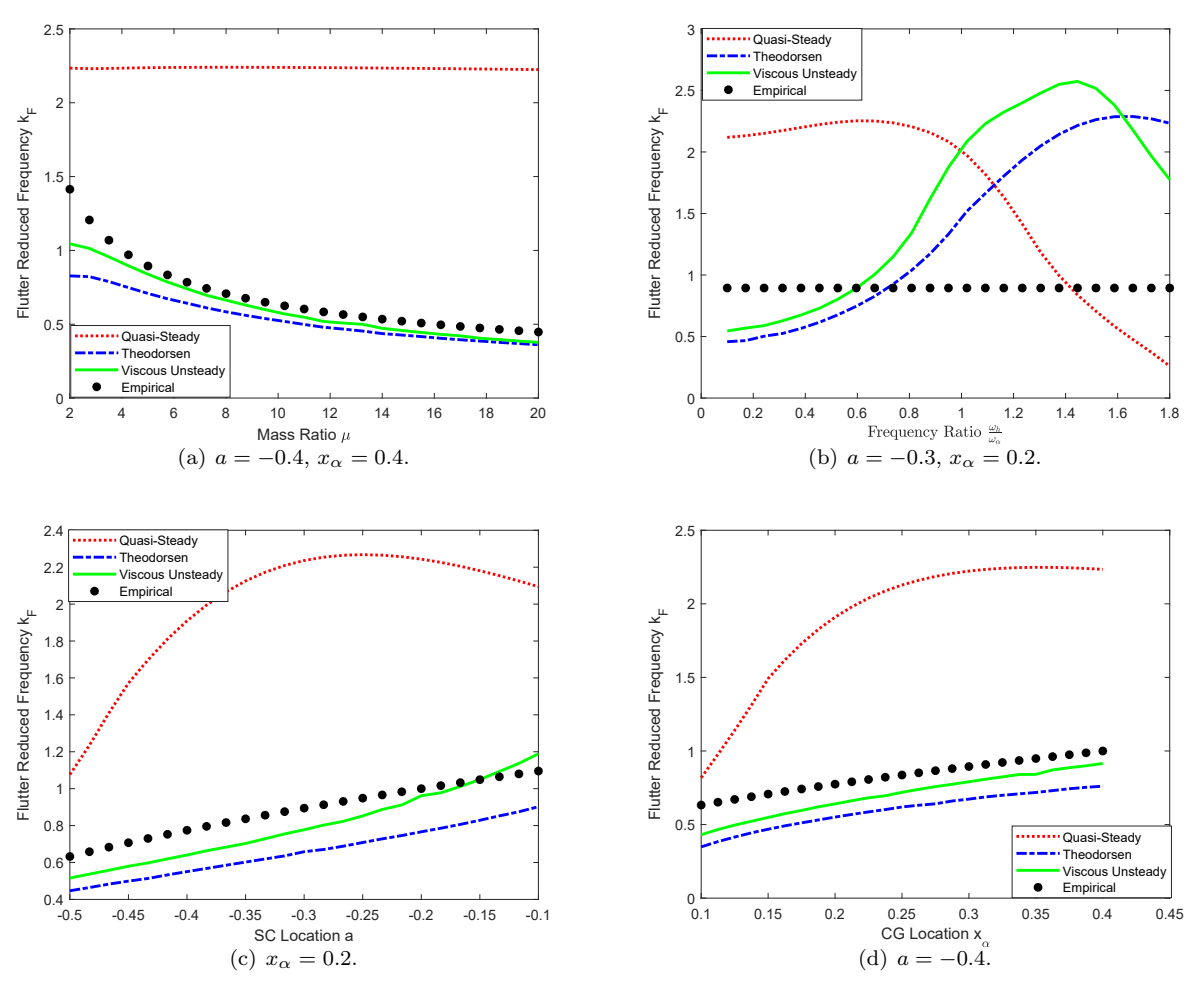


Figure 10: Variation of flutter reduced frequency k_F with the section parameters.

which is expected. Moreover, the inviscid unsteady theory fails to predict flutter at negative values of x_{α} ; it has been known that a center of gravity forward of the shear center precludes flutter. However, the viscous theory asserts the existence of flutter at this forward cg location, yet with large speeds and low frequencies. As discussed above, this is a serious finding as it points to the inadequacy of Theodorsen's theory to capture flutter in situations where it exists, which was encountered by earlier researchers. Even at backward cg locations where the inviscid unsteady theory captures a flutter boundary, it is considerably deviated (higher) from the viscous boundary: more than 25% deviation in flutter speed and 30% deviation in frequency.

x_{α}	Quasi-Steady		Theodorsen		Viscous Unsteady	
	$\frac{U_F}{b\omega_{\alpha}}$	k_F	$\frac{U_F}{b\omega_{\alpha}}$	k_F	$\frac{U_F}{b\omega_{\alpha}}$	k_F
-0.1	0.51	1.97	No Flutter		4.64	0.18
0	Unstable		1.41	0.55	1.13	0.71
0.1	0.24	4.16	0.89	0.90	0.7	1.23

Table 1: Comparison for the flutter boundary at different values of x_{α} (cg locations) using (i) quasi-steady aerodynamics, (ii) inviscid unsteady aerodynamics, ⁹ and (iii) the developed viscoud unsteady aerodynamic theory.

V. Conclusion

In this paper, we demonstrate our recently developed viscous extension of the classical theory of unsteady aerodynamics. In this theory, we relax the Kutta condition and induce a pressure singularity at the trailing edge; we determine the strength of such a singularity by extending the triple deck boundary layer theory, thereby providing a viscous correction to the unsteady lift. Based on this theory, a viscous (Reynoldsnumber-dependent) frequency response is developed. That is, the inviscid Theodorsen function is extended to the viscous case. It is found that viscosity induces a significant phase lag to the lift development beyond Theodorsen's inviscid solution, particularly at high frequencies and low Reynolds numbers, which is expected to significantly affect the flutter boundary. To show that, couple the newly developed viscous unsteady aerodynamic theory with a structural dynamic model of a typical section to perform aeroelastic simulation and analysis. It is found that the inviscid flutter boundary using Theodorsen's theory is non-conservative: it fails to capture the flutter boundary in cases where flutter exists, which was encountered by earlier researchers. Moreover, even in the cases where Theodorsen's theory captures a flutter boundary, it is typically higher than the viscous boundary. This finding has serious consequences because it will jeopardize design of air vehicles based on Theodorsen's theory: they can be susceptible to flutter.

Acknowledgments

The authors would like to acknowledge the NSF grant CMMI-1635673.

References

¹Bisplinghoff, R. L., Ashley, H., and Halfman, R. L., Aeroelasticity, Dover Publications, New York, 1996.

²Nayfeh, A. H. and Pai, P. F., *Linear and nonlinear structural mechanics*, John Wiley & Sons, 2004.

³Hodges, D. H., "Nonlinear composite beam theory," Progress in astronautics and aeronautics, Vol. 213, 2006, pp. 304.

⁴Katz, J. and Plotkin, A., Low-speed aerodynamics, Cambridge University Press, 2001.

⁵Taha, H. and Rezaei, A. S., "Viscous Extension of Potential-Flow Unsteady Aerodynamics: The Lift Frequency Response Problem," Under Review in the Journal of Fluid Mechanics, 2018.

⁶Birnbaum, W., "Der Schlagflugelpropeller und die Kleinen Schwingungen elastisch befestigter Tragflugel," Z Flugtech Motorluftschiffahrt, Vol. 15, 1924, pp. 128–134.

⁷Prandtl, L., "Über die Entstehung von Wirbeln in der idealen Flüssigkeit, mit Anwendung auf die Tragflügeltheorie und andere Aufgaben," *Vorträge aus dem Gebiete der Hydro-und Aerodynamik (Innsbruck 1922)*, Springer, 1924, pp. 18–33.

⁸Wagner, H., "Uber die entstehung des dynamischen auftriebs von tragflugeln," ZAMM, Vol. 5, 1925.

⁹Theodorsen, T., "General Theory of Aerodynamic Instability and the Mechanism of Flutter," Tech. Rep. 496, NACA, 1935.

¹⁰Von Karman, T. and Sears, W. R., "Airfoil theory for non-uniform motion." J. Aeronautical Sciences, Vol. 5, No. 10, 1938, pp. 379–390

¹¹Küssner, H. G., "Schwingungen von Flugzeugflügeln," Jahrbuch der deutscher Versuchsanstalt für Luftfahrt especially Section E3 Einfluss der Baustoff-Dämpfung, 1929, pp. 319–320.

- ¹²Schwarz, L., "Brechnung der Druckverteilung einer harmonisch sich Verformenden Tragflache in ebener Stromung," Vol. 17, Luftfahrtforsch, Dec 1940.
- ¹³Loewy, R. G., "A two-dimensional approximation to unsteady aerodynamics in rotary wings," *Journal of Aeronautical Sciences*, Vol. 24, 1957, pp. 81–92.
- ¹⁴Jones, M. A., "The separated flow of an inviscid fluid around a moving flat plate," *Journal of Fluid Mechanics*, Vol. 496, 2003, pp. 405–441.
- ¹⁵Yongliang, Y., Binggang, T., and Huiyang, M., "An analytic approach to theoretical modeling of highly unsteady viscous flow excited by wing flapping in small insects," *Acta Mechanica Sinica*, Vol. 19, No. 6, 2003, pp. 508–516.
- ¹⁶Pullin, D. I. and Wang, Z., "Unsteady forces on an accelerating plate and application to hovering insect flight," *Journal of Fluid Mechanics*, Vol. 509, 2004, pp. 1–21.
- ¹⁷Ansari, S. A., Żbikowski, R., and Knowles, K., "Non-linear unsteady aerodynamic model for insect-like flapping wings in the hover. Part 1: methodology and analysis," *Proceedings of the Institution of Mechanical Engineers, Part G: Journal of Aerospace Engineering*, Vol. 220, No. 2, 2006, pp. 61–83.
- ¹⁸Michelin, S. and Smith, S. G. L., "An unsteady point vortex method for coupled fluid-solid problems," *Theoretical and Computational Fluid Dynamics*, Vol. 23, No. 2, 2009, pp. 127–153.
- ¹⁹Tchieu, A. A. and Leonard, A., "A discrete-vortex model for the arbitrary motion of a thin airfoil with fluidic control," *Journal of Fluids and Structures*, Vol. 27, No. 5, 2011, pp. 680–693.
- ²⁰Wang, C. and Eldredge, J. D., "Low-order phenomenological modeling of leading-edge vortex formation," *Theoretical and Computational Fluid Dynamics*, Vol. 27, No. 5, 2013, pp. 577–598.
- ²¹Ramesh, K., Gopalarathnam, A., Edwards, J. R., Ol, M. V., and Granlund, K., "An unsteady airfoil theory applied to pitching motions validated against experiment and computation." *Theoretical and Computational Fluid Dynamics*, 2013, pp. 1–22.
- ²²Ramesh, K., Gopalarathnam, A., Granlund, K., Ol, M. V., and Edwards, J. R., "Discrete-vortex method with novel shedding criterion for unsteady aerofoil flows with intermittent leading-edge vortex shedding," *Journal of Fluid Mechanics*, Vol. 751, 2014, pp. 500–538.
- ²³Yan, Z., Taha, H., and Hajj, M. R., "Geometrically-Exact Unsteady Model for Airfoils Undergoing Large Amplitude Maneuvers," Aerospace Science and Technology, Vol. 39, 2014, pp. 293–306.
- ²⁴Li, J. and Wu, Z.-N., "Unsteady lift for the Wagner problem in the presence of additional leading/trailing edge vortices," Journal of Fluid Mechanics, Vol. 769, 2015, pp. 182–217.
- ²⁵Hussein, A. A., Hajj, M. R., Elkholy, S. M., and ELbayoumi, G. M., "Dynamic Stability of Hingeless Rotor Blade in Hover Using Padé Approximations," AIAA Journal, 2016, pp. 1769–1777.
- ²⁶Hussein, A. A. and Canfield, R. A., "Unsteady Aerodynamic Stabilization of the Dynamics of Hingeless Rotor Blades in Hover," AIAA Journal, Vol. 56, No. 3, 2017, pp. 1298–1303.
- ²⁷Hussein, A., Ragab, S. A., Taha, H. E., and Hajj, M. R., "Optimal Tail Kinematics for Fish-Like Locomotion using the Unsteady Vortex Lattice Method," 2018 AIAA Aerospace Sciences Meeting, 2018, p. 0311.
- ²⁸Crighton, D. G., "The Kutta condition in unsteady flow," Annual Review of Fluid Mechanics, Vol. 17, No. 1, 1985, pp. 411–445.
- ²⁹Howarth, L., "The theoretical determination of the lift coefficient for a thin elliptic cylinder," *Proceedings of the Royal Society of London. Series A, Mathematical and Physical Sciences*, Vol. 149, No. 868, 1935, pp. 558–586.
- ³⁰Basu, B. C. and Hancock, G. J., "The unsteady motion of a two-dimensional aerofoil in incompressible inviscid flow," *Journal of Fluid Mechanics*, Vol. 87, No. 01, 1978, pp. 159–178.
- ³¹Daniels, P. G., "On the unsteady Kutta condition," The Quarterly Journal of Mechanics and Applied Mathematics, Vol. 31, No. 1, 1978, pp. 49–75.
- ³²Satyanarayana, B. and Davis, S., "Experimental studies of unsteady trailing-edge conditions," AIAA Journal, Vol. 16, No. 2, 1978, pp. 125–129.
- ³³Bass, R. L., Johnson, J. E., and Unruh, J. F., "Correlation of lift and boundary-layer activity on an oscillating lifting surface," *AIAA Journal*, Vol. 20, No. 8, 1982, pp. 1051–1056.
 - ³⁴Rott, N. and George, M. B. T., "An Approach to the Flutter Problem in Real Fluids," Tech. Rep. 509, 1955.
- $^{35}\mathrm{Abramson},$ H. N. and Chu, H.-H., "A discussion of the flutter of submerged hydrofoils," Journal of Ship Research, Vol. 3, No. 2, 1959.
 - ³⁶Henry, C. J., "Hydrofoil Flutter Phenomenon and Airfoil Flutter Theory," Tech. Rep. 856, Davidson Laboratory, 1961.
- ³⁷Chu, W.-H., "An aerodynamic analysis for flutter in Oseen-type viscous flow," *Journal of the Aerospace Sciences*, Vol. 29, 1961, pp. 781–789.
- ³⁸Shen, S. F. and Crimi, P., "The theory for an oscillating thin airfoil as derived from the Oseen equations," *Journal of Fluid Mechanics*, Vol. 23, No. 03, 1965, pp. 585–609.
- ³⁹Woolston, D. S. and Castile, G. E., "Some effects of variations in several parameters including fluid density on the flutter speed of light uniform cantilever wings," Tech. Rep. 2558, NACA, 1951.
- ⁴⁰Chu, W.-H. and Abramson, H. N., "An Alternative Formulation of the Problem of Flutter in Real Fluids," *Journal of the Aerospace Sciences*, Vol. 26, No. 10, 1959.
- ⁴¹Abramson, H. N., Chu, W.-H., and Irick, J. T., "Hydroelasticity with special reference to hydrofoil craft." Tech. Rep. 2557, NSRDC Hydromechanics Lab, 1967.
- ⁴²Savage, S. B., Newman, B. G., and Wong, D. T.-M., "The role of vortices and unsteady effects during the hovering flight of dragonflies," *The Journal of Experimental Biology*, Vol. 83, No. 1, 1979, pp. 59–77.
- ⁴³Orszag, S. A. and Crow, S. C., "Instability of a Vortex Sheet Leaving a Semi-Infinite Plate," *Studies in Applied Mathematics*, Vol. 49, No. 2, 1970, pp. 167–181.

- ⁴⁴Ansari, S. A., Zbikowski, R., and Knowles, K., "Non-linear Unsteady Aerodynamic Model for Insect-Like Flapping Wings in the Hover. Part2: Implementation and Validation," *Journal of Aerospace Engineering*, Vol. 220, 2006, pp. 169–186.
- ⁴⁵Pitt Ford, C. W. and Babinsky, H., "Lift and the leading-edge vortex," *Journal of Fluid Mechanics*, Vol. 720, 2013, pp. 280–313.
- ⁴⁶Hemati, M. S., Eldredge, J. D., and Speyer, J. L., "Improving vortex models via optimal control theory," *Journal of Fluids and Structures*, Vol. 49, 2014, pp. 91–111.
- ⁴⁷Zakaria, M. Y., Taha, H. E., and Hajj, M. R., "Design optimization of flapping ornithopters: the pterosaur replica in forward flight," *Journal of Aircraft*, Vol. 53, No. 1, 2015, pp. 48–59.
- ⁴⁸Taha, H. and Rezaei, A. S., "Unsteady Viscous Lift Frequency Response Using The Triple Deck Theory," AIAA-Paper 2018-0038.
- ⁴⁹Abramson, H. N. and Ransleben, G. E., "An experimental investigation of flutter of a fully submerged subcavitating hydrofoil," *Journal of Aircraft*, Vol. 2, No. 5, 1965, pp. 439–442.
 - ⁵⁰Schlichting, H., Gersten, K., Krause, E., Oertel, H., and Mayes, K., Boundary-layer theory, Vol. 7, Springer, 1955.
 - ⁵¹Blasius, H., Grenzschichten in Flüssigkeiten mit kleiner Reibung, Druck von BG Teubner, 1908.
- ⁵²Goldstein, S., "Concerning some solutions of the boundary layer equations in hydrodynamics," *Mathematical Proceedings* of the Cambridge Philosophical Society, Vol. 26, No. 1, 1930, pp. 1–30.
- ⁵³Lighthill, M. J., "On boundary layers and upstream influence. II. Supersonic flows without separation," *Proceedings of the Royal Society of London A: Mathematical, Physical and Engineering Sciences*, Vol. 217, No. 1131, 1953, pp. 478–507.
- ⁵⁴Brown, S. N. and Daniels, P. G., "On the viscous flow about the trailing edge of a rapidly oscillating plate," *Journal of Fluid Mechanics*, Vol. 67, No. 04, 1975, pp. 743–761.
- ⁵⁵Messiter, A. F., "Boundary-layer flow near the trailing edge of a flat plate," SIAM Journal on Applied Mathematics, Vol. 18, No. 1, 1970, pp. 241–257.
- ⁵⁶Stewartson, K., "On the flow near the trailing edge of a flat plate," Proceedings of the Royal Society of London A: Mathematical, Physical and Engineering Sciences, Vol. 306, No. 1486, 1968, pp. 275–290.
 - ⁵⁷Brown, S. N. and Stewartson, K., "Trailing-edge stall," Journal of Fluid Mechanics, Vol. 42, No. 03, 1970, pp. 561–584.
- ⁵⁸Chow, R. and Melnik, R. E., "Numerical solutions of the triple-deck equations for laminar trailing-edge stall," *Proceedings* of the Fifth International Conference on Numerical Methods in Fluid Dynamics June 28–July 2, 1976 Twente University, Enschede, Springer, 1976, pp. 135–144.
- ⁵⁹Brown, S. N. and Cheng, H. K., "Correlated unsteady and steady laminar trailing-edge flows," *Journal of Fluid Mechanics*, Vol. 108, 1981, pp. 171–183.
 - ⁶⁰Schlichting, H. and Truckenbrodt, E., Aerodynamics of the Airplane, McGraw-Hill, 1979.
 - ⁶¹Robinson, A. and Laurmann, J. A., Wing theory, Cambridge University Press, 1956.
- ⁶²Rezaei, A. S. and Taha, H., "Computational Study of Lift Frequency Responses of Pitching Airfoils at Low Reynolds Numbers," AIAA-Paper 2017-0716, 2017.
- ⁶³Othman, M., Ahmed, M. Y., and Zakaria, M. Y., "Investigating the Aerodynamic Loads and Frequency Response for a Pitching NACA 0012 Airfoil," 2018 AIAA Aerospace Sciences Meeting, 2018, p. 0318.
- ⁶⁴Theodorsen, T. and Garrick, I. E., "Mechanism of flutter a theoretical and experimental investigation of the flutter problem," Tech. Rep. 685, NATIONAL AERONAUTICS AND SPACE ADMINISTRATION WASHINGTON DC, 1940.